

MSTAR: A FORTRAN Program for the Model Independent Molecular Weight Analysis of Macromolecules using Low Speed or High Speed Sedimentation Equilibrium

By S.E. Harding, J.C. Horton and P.J. Morgan

UNIVERSITY OF NOTTINGHAM, DEPARTMENT OF APPLIED BIOCHEMISTRY AND FOOD SCIENCE, SUTTON BONINGTON, LE12 5RD U.K.

1. INTRODUCTION

Besides conformational and homogeneity analyses, the principle use of the analytical ultracentrifuge is for the absolute (*i.e.* not requiring calibration standards) measurement of molecular weight and related parameters (such as interaction constants and thermodynamic non-ideality coefficients). There is currently a range of software that has been produced by users of the ultracentrifuge over the years for this purpose. This ranges from simple linear regression analysis of log concentration *versus* radial displacement squared plots from the sedimentation equilibrium of well-behaved single solute protein systems right through to software for the analysis of complicated self-associating and non-ideal systems. For example, the FORTRAN programs BIOSPIN and NONLIN from the laboratory of David Yphantis at Storrs, Connecticut, have been very popular for this purpose.

In our laboratory at Nottingham, we have been using various forms of a program called MSTAR for the molecular weight analysis of systems of macromolecules from sedimentation equilibrium patterns recorded using the Rayleigh interference and absorption optical systems of an analytical ultracentrifuge. It derives from an early program written by Michael Creeth - then at the University of Bristol - for a Wang desk-top calculator and later extended and adapted for mainframe FORTRAN by one of us (SEH). These versions were for the analysis of a relatively limited number of data points recorded from Rayleigh fringe profiles using manually operated microcomparators. It has now been recently adapted by us to the case of Rayleigh interference data captured semi-automatically *off-line* from the Beckman Model E *via* a laser densitometer gel scanner (see Chapter 5 of this volume) and also to the case of absorption data captured *on-line* from the Beckman Optima XL-A.

MSTAR serves two purposes:

- (i) First, for a finite loading concentration, it will estimate the (apparent) *whole cell* weight average molecular weight ($M_{w,app}^0$) using a procedure involving an operational point average molecular weight, M^* : this procedure appears particularly well suited for the analysis of difficult heterogeneous systems.
- (ii) Secondly, it estimates apparent *point* weight average molecular weights as a function of the square of the radial displacement (or equivalently point concentration). Providing the initial fringe or absorbance data is of sufficient quality, it will then estimate point z-average molecular weight and the Roark-Yphantis¹ M_{y2} point average (a "compound" average, free of first order effects of non-ideality).

Purpose (ii) resembles a similar objective of the Yphantis program BIOSPIN^{2,3} although (i) is different. It also has a facility for evaluating meniscus concentrations, useful for the evaluation of low speed sedimentation equilibrium solute distributions recorded using the Rayleigh interference optical system. MSTAR does not assume any model (monodisperse, monomer-dimer, Gaussian distribution, *etc.*) and hence is different from programs like NONLIN^{2,3} for the analysis of non-ideal self-associations and our own POLY for the analysis of non-ideal systems which are polydisperse in a discrete (as opposed to quasi-continuous) sense.

In this Chapter we will describe the two versions of MSTAR: MSTAR1 (for the analysis of sedimentation equilibrium solute distributions recorded using the Rayleigh interference optical system) and MSTARA (for distributions recorded using absorption optics). Although in their current form they have been written for a mainframe computer (with graphics peculiar to the IBM/3084Q at the University of Cambridge), it is expected that both forms will be available for a PC in the near future.

2. MOLECULAR WEIGHT PARAMETERS SOUGHT

Although all three principle molecular weight averages, M_n , M_w and M_z , are in theory extractable, because the bulk of our work in the past has involved the use of the Rayleigh optical system and because we have been looking at highly polydisperse systems - such as polysaccharides which are not well suited for using the meniscus depletion method - number averages have not been readily obtainable* and hence we have focussed almost exclusively on the extraction of weight average molecular weights, and - to a lesser extent - on z-average molecular weights. Although the low-speed method for many systems of macromolecules is more suitable, only the high-speed method readily yields number average molecular weight data - for the latter BIOSPIN is recommended.

* A method for the evaluation of $M_n(a)$, the point average molecular weight is normally required.

Point Average Molecular Weights

The simplest molecular weight parameter to come out of sedimentation equilibrium analysis, if Rayleigh or absorption optics are used, is the apparent point weight average molecular weight, $M_{w,app}(r)$ defined by⁵

$$M_{w,app}(r) = \frac{1}{k} \frac{d \ln C(r)}{d(r^2)} \quad (1a)$$

where $C(r)$ is the concentration (g/ml) at a radial position r and k is a run constant given by

$$k = \frac{(1-\bar{v}\rho)\omega^2}{2RT} \quad (2)$$

where ω is the angular velocity of the rotor (rads/sec), R is the gas constant, T the absolute temperature, \bar{v} the partial specific volume of the macromolecular solute (in ml/g) and ρ the solution density (in g/ml)[†]. The reason why the molecular weight in eq. (1) is an *apparent* one is that it corresponds to a finite concentration C . If absorption optics are used, then within the validity of the Lambert-Beer equation

$$A = \epsilon_\lambda Cl \quad (3)$$

[where ϵ_λ is the extinction coefficient ($\text{ml.g}^{-1}.\text{cm}^{-1}$), and l the cell path length (cm)], the absorbance, A , at a given wavelength, λ is proportional to C and hence

$$M_{w,app}(r) = \frac{1}{k} \frac{d \ln A}{d(r^2)} \quad (1b)$$

If Rayleigh optics are used, the fringe displacement, J is also proportional to C :

$$J = \frac{\mathcal{R}C}{\lambda} \quad (4)$$

(cf. eqs. (2.5) and (2.6) of ref. 5) where \mathcal{R} is the specific refraction increment (ml.g^{-1}). Unfortunately unless the meniscus depletion method is employed, Rayleigh interference patterns yield directly fringe displacements *only relative to the meniscus*⁵, and we denote these relative fringe displacements by $j(r)$, where

$$j(r) = J(r) - J_a \quad (5)$$

J_a being the meniscus fringe number. The form of eq. (1) for Rayleigh optics is therefore⁵

$$M_{w,app}(r) = \frac{1}{k} \frac{d \ln J}{d(r^2)} \equiv \frac{1}{k} \frac{d \ln (j + J_a)}{d(r^2)} \quad (1c)$$

There are various ways of extracting J_a (or equivalently C_a): MSTAR1 uses a fairly simple procedure which is summarised in section 3 below.

[†] In practice, the solvent density can be used: this significantly affects only the interpretation of virial coefficient information and can be positively advantageous (see Chapter 17 this volume and ref. 4, pp. 284-285).

To obtain point z-average molecular weights, $M_{z,app}(r)$, an estimate for the meniscus concentration is *not* required, even for distributions recorded using Rayleigh optics. However a double derivative of the fringe data *is* required:

$$M_{z,app}(r) = M_{w,app}(r) + \frac{1}{k} \left\{ \frac{d \ln M_{w,app}(r)}{d(r^2)} \right\} \quad (6a)$$

$$\equiv \frac{1}{k} \frac{d}{d(r^2)} \left(\ln \left\{ \frac{1}{r} \frac{dC(r)}{dr} \right\} \right) \quad (6b)$$

(*cf* eqs. (2.12) and (2.42) of ref. 5) and so data of a high quality is usually needed, unless heavy data smoothing routines are employed.

It is possible also to define another derived or "compound" point average. This is the Roark-Yphantis¹ M_{y2} point average, which is free from first order effects of thermodynamic non-ideality:

$$M_{y2}(r) = \frac{M_{w,app}^2(r)}{M_{z,app}(r)} \quad (7)$$

Whole Cell Weight Average Molecular Weight

Arguably the most useful - at least the most basic - parameter to derive from sedimentation equilibrium analysis is the (apparent) average molecular weight for the distribution of solute averaged over all radial positions in the solution column of the cell, $M_{w,app}^0$. This is conventionally obtained by estimating an average slope of a plot of $\log C$ versus r^2 , or equivalently, from determination of the concentrations of solute at the cell meniscus ($r=a$) and base ($r=b$), C_a , C_b respectively, and from knowledge of the initial loading concentration C_0 :

$$M_{w,app}^0 = \frac{1}{k(b^2-a^2)} \left\{ \frac{C_b - C_a}{C_0} \right\} \quad (8)$$

where the concentrations could either be on a weight basis, in terms of absorbance (with the limits of the Lambert-Beer law) or in terms of absolute Rayleigh fringe displacements, J . For simple, well behaved, monodisperse, approximately ideal solutes this equation gives adequate (*i.e.* to within $\pm 5\%$) estimates for $M_{w,app}^0$ (provided that the term $\bar{v}\rho$ in eq. (2) is not too close to unity). For heterogeneous solutions, particularly where there is strong curvature in the $\log C$ versus r^2 plots (especially if Rayleigh optics are being employed), and also if the optical records near the cell base are not clearly defined, estimates for C_b can be very difficult to obtain with any reasonable precision. We find a useful way of minimising these problems is to use an operational point average, M^* . M^* can be found from Rayleigh or absorption sedimentation equilibrium records *via* the relation

$$\frac{C(r) - C_a}{M^*(r)} = kC_a (r^2 - a^2) + 2k \int_a^r r [C(r) - C_a] dr \quad (9)$$

Several years ago⁷ Michael Creeth and one of us (SEH) explored the properties of M^* in some detail and found it to have some useful features, one of which is that at the cell base $M^* = M_{w,app}^0$: as is pointed out later in Chapter 27 of this volume, use of M^* generally provides a better way of estimating $M_{w,app}^0$ compared to the conventional use of eq. (8) (see Table 1 of Chapter 27). Further, an independent estimate of the initial cell loading concentration, C_0 is *not* required. As the name implies, it is this M^* function which forms the basis of MSTARI and MSTARA.

The M^* function provides no improvement on obtaining whole cell z-average molecular weights, $M_{z,app}^0$ so the current versions of MSTAR don't evaluate this.

Reduced Molecular Weights

Optical records from sedimentation equilibrium do not yield molecular weights directly but *reduced* (apparent) molecular weights, A_i^\dagger , defined by

$$A_i = k M_{app,i} \quad (10)$$

(*cf.* eqs. (1), (6) and (8)) where k is given by eq. (2), and where the subscript i can represent point number, weight, z or y_2 averages, or the whole-cell weight average, or the star operational average (eq. (8)). We use the symbol A_i for reduced averages following the original convention of Rinde⁸. Another popular alternative is the use of "reduced moments", σ_i , where $\sigma_i = 2A_i$ (see *e.g.* Chapters 7 and 13 of this volume), although, since our main focus of attention has been on polydisperse macromolecules like polysaccharides and glycoconjugates, we prefer to use the Rinde notation to avoid confusion of σ with standard deviations of molecular weight distributions.

3. DETERMINATION OF MENISCI CONCENTRATIONS

For the evaluation of point weight average molecular weights and whole cell weight average molecular weights from Rayleigh interference optical records, and also for the evaluation of whole cell weight average molecular weights from absorption optical records it is necessary to estimate the solute concentration at the meniscus, C_a (or equivalently, for Rayleigh optics, J_a).

C_a from Absorption Optical Records

Fortunately if the absorption system is used this is usually trivial, since absorption is a direct record of solute concentration within the Lambert-Beer range. A simple linear extrapolation to the meniscus usually suffices: even for cases where a long extrapolation has been necessary (due to errors in cell filling), this extrapolation has given reasonable results.

* Note that the symbol A is used for absorbance whereas the symbol for reduced molecular weight is A_i (*i.e.* with a subscript or superscript).

C_a (or J_a) from Rayleigh Optical Records

As has been well reported in the past, this is unfortunately not as easy since the optical records are a direct record of *relative* concentrations. Creeth and Pain⁵ considered a whole variety of procedures for extracting J_a . We have generally used a procedure described in ref. 7; we will give an outline of it here.

One of the forms of the fundamental equation of sedimentation equilibrium is

$$\frac{J(r)}{A_n(r)} - \frac{J_a}{A_n(a)} = 2 \int_a^r rJ \, dr \quad (11)$$

(see e.g. eqs. (8) and (26) of ref. 6). Creeth⁹ suggested a new variable, $A^*(r)$, be identified by writing

$$\frac{j(r)}{A^*(r)} \equiv \frac{J(r)}{A_n(r)} - \frac{J_a}{A_n(a)} \quad (12)$$

Substituting eq. (12) and eq. (5) into eq. (11) gives

$$\frac{j(r)}{A^*(r)} = J_a(r^2 - a^2) + 2 \int_a^r rj \, dr \quad (13)$$

A further re-arrangement gives

$$\frac{j(r)}{(r^2 - a^2)} = J_a A^*(r) + \frac{2 A^*(r)}{(r^2 - a^2)} \int_a^r rj \, dr \quad (14)$$

Thus a plot of $j(r)/(r^2 - a^2)$ against $I(r)/(r^2 - a^2)$, where $I(r)$ is defined by

$$I(r) \equiv \int_a^r rj \, dr \quad (15)$$

gives an intercept at $r=a$ of $J_a A^*(a)$ and a limiting slope at $r=a$ of $2A^*(a)$. Hence

$$J_a = \frac{2 \times \text{intercept at } r=a}{\text{slope at } r=a} \quad (16)$$

The integral can be evaluated using a standard numerical package (in the case of MSTARI this is the NAG (Numerical Algorithms Group, Oxford, UK) routine D01GAF as will be described below. A similar procedure has been given by Teller *et al.*¹⁰.

For systems that are fairly ideal and monodisperse such a plot is approximately linear (Fig. 1a) and extraction of J_a is therefore easy. For other systems however it is not linear and the functional form of the integral in eq. (15) is not known (Fig. 1b). Two opposing criteria have to be taken into account: (i) because a limiting slope is required at the meniscus, *greater weight* should be paid towards those data nearer the meniscus; (ii) unfortunately, as is well known, fringe displacement data are not

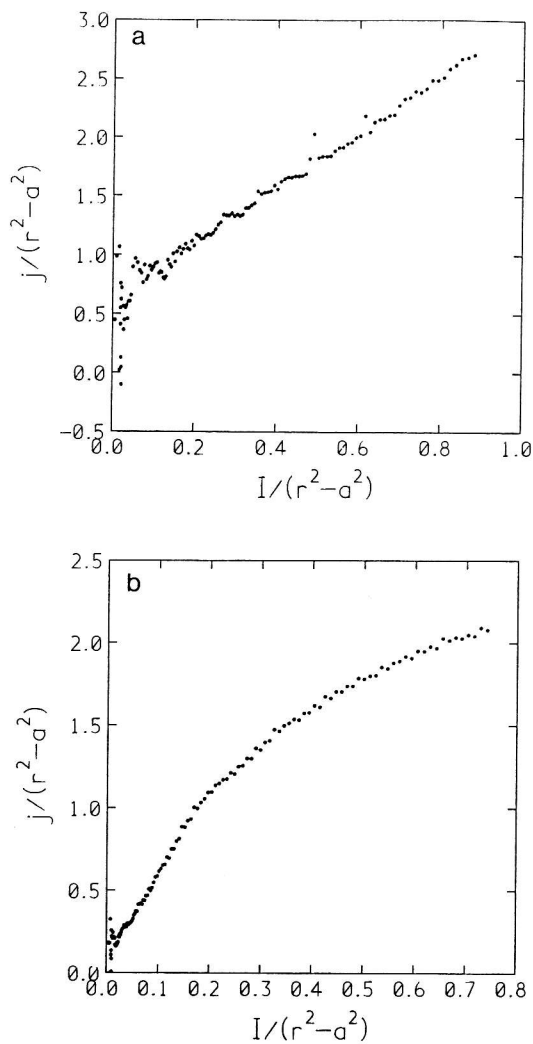


Figure 1. MSTAR $j/(r^2-a^2)$ versus

$$\frac{1}{(r^2-a^2)} \int_a^r rj \, dr$$

plots for sedimentation runs (recorded using the Rayleigh interference optical system on a Beckman Model E) on (a) a fairly homogeneous/ideal solution of colonic mucin "T-domains" ($J_a \sim 0.58 \pm 0.05$); (b) a highly non-ideal solution of xanthan ("RD") ($J_a \sim 0.01 \pm 0.01$ i.e. near meniscus depletion conditions).

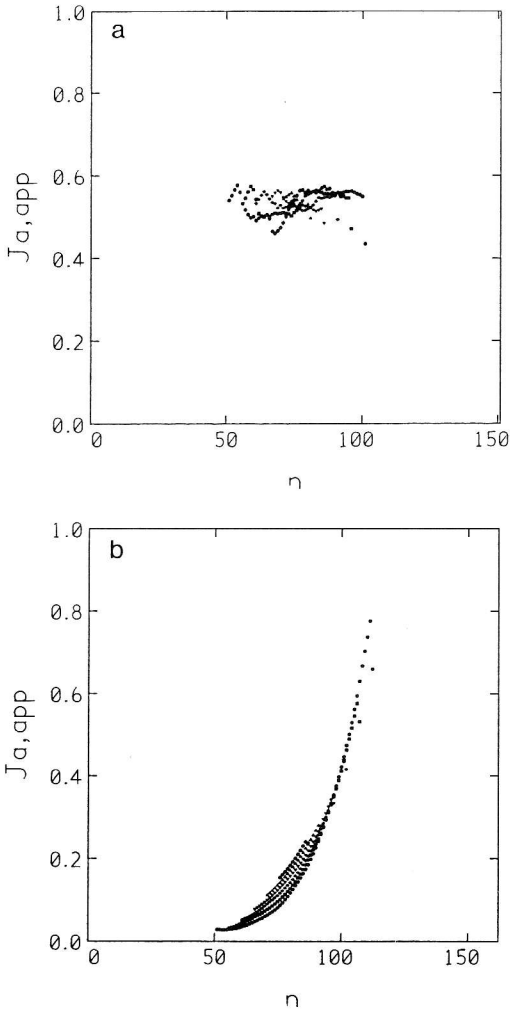


Figure 2. MSTARI plots of apparent meniscii concentrations ($J_{a,app}$) as a function of radial position number, n from sedimentation equilibrium solute distributions (in aqueous solvents) of (a) colonic mucin "T-domains" and (b) xanthan where $n = \{(r-a)/(b-a)\} N_{TOT}$ and N_{TOT} is the total number of experimental points (at equal intervals of radial distance, r) between a and b .

accurate near the meniscus and so *less weight* should be applied. This apparent dilemma is offset by the facility of having large amounts of fringe data from automatic (off- or on-line) data capture, and so in practice what we do is to use a sliding strip procedure which is iterated along the $j/(r^2-a^2)$ versus $I/(r^2-a^2)$ curve, the procedure repeated for several sliding strip lengths. These estimates for J_a (" $J_{a,app}$ ") can then be extrapolated to zero meniscus position to give an "ideal" J_a value (Fig. 2). The procedure usually works well even for very heterogeneous systems (Fig. 2b).

We will now consider in turn the two versions MSTARA and MSTAR of MSTAR. We will consider MSTARA first since it is easy to implement (no problems of J_a estimates).

4. MSTARA

Evaluation of the Integral, $I(r)$

$I(r)$ is evaluated *via* eq. (15) by employing the NAG routine D01GAF. D01GAF is a method due to Gill and Miller¹¹ for integrating a function of which at least four data points are known. In the XL-A implementation of this program, the first data point is $r=r_1$ ($>a$). In such cases $I(r)$ is split into two parts: from a to r_1 and from r_1 to r . The second part is evaluated with D01GAF and the first part (which, in fact, is usually quite small compared with the second part) with a simple linear extrapolation (see Appendix). The whole procedure is summarised in Fig. 3. Once I has been evaluated, M^* can then be readily calculated and an example of a plot of M^* versus the radial displacement squared parameter, ξ (together with the corresponding plot of $\ln A$ versus ξ) is given for IgM in Fig. 4 where

$$\xi = \frac{r^2 - a^2}{b^2 - a^2} \quad (17)$$

Point Weight Average Molecular Weight

We can now return to the calculation of the point (apparent) weight average molecular weight *i.e.* $M_{w,app}(r)$. Values of $M_{w,app}(r)$ are calculated by considering sliding strips of consecutive $(r^2, \ln J)$ data points and calculating the slope of the sliding strip at the middle point. (Sliding strips are always chosen so that they contain an odd number of points. This is ensured by defining their length to be $2w+1$ where w is an integer. As will be seen below, this is convenient since w has a natural meaning in this method). This slope calculation is done using three NAG routines. First, E02ADF (which uses Chebyshev polynomials) is called to fit a quadratic line to the data points. This is the process referred to as FIT in Fig. 5. Next the fitted line is differentiated (in its Chebyshev representation) with E02AHF - DIFF in Fig. 5. Finally, since both the line and its differential are still in the form of sums of Chebyshev polynomials, E02AEF is called to evaluate them at the middle point of the strip. For the sake of completeness, the residuals (*i.e.* the differences between the actual data points and the fits) were also calculated (RESID in Fig. 5). Fig. 5 is a flow diagram summarising the

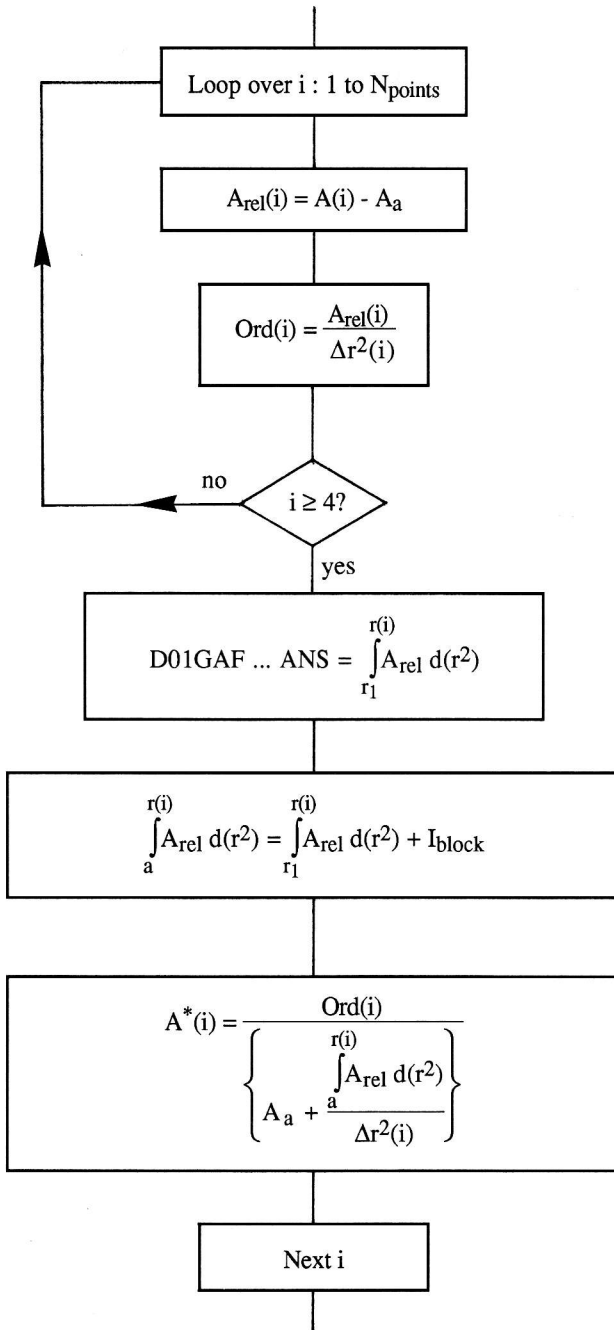


Figure 3. Calculation of A^* (and hence M^*). I_{block} is defined in the appendix.

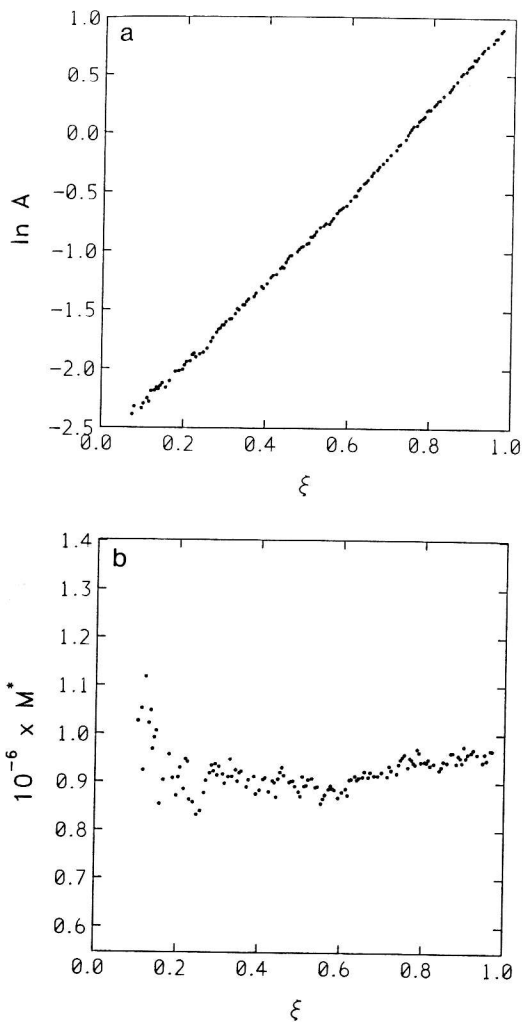


Figure 4. MSTARA (a) $\ln A$ versus ξ and (b) corresponding M^* versus ξ plots from a low speed sedimentation equilibrium experiment (recorded using the absorption optical system on the Beckman Optima XL-A) on human IgM₁ in phosphate/chloride buffer (pH=6.8, ionic strength, I=0.1) at a loading concentration of ~0.6 mg/ml. Scanning wavelength = 278 nm. Rotor speed = 5000 rev/min; temperature = 20.0°C. $M_w^0 \sim M_w^0 = M^*(\xi \rightarrow 1)$ (from plot (b)) = $(1.00 \pm 0.02) \times 10^6$ g/mol.

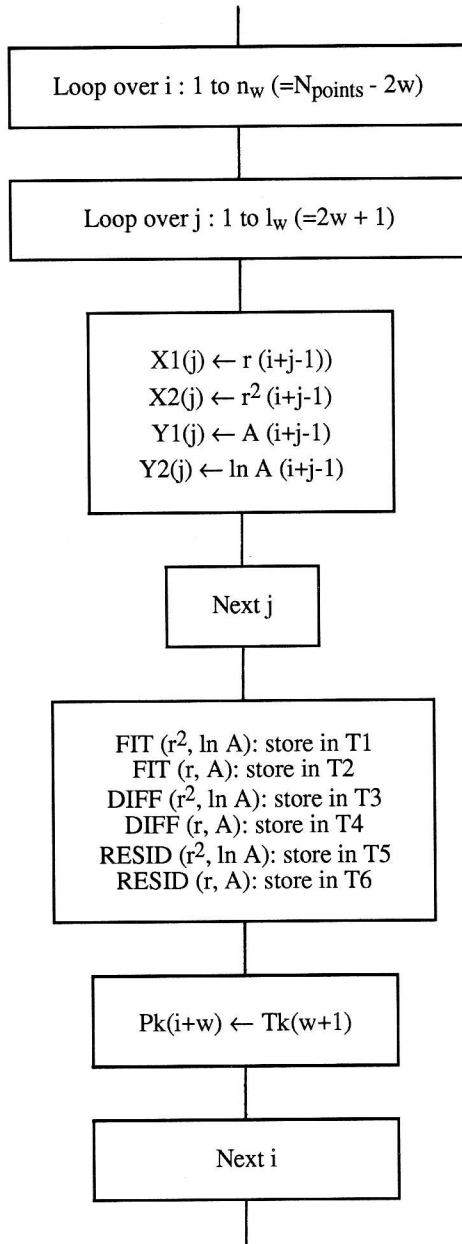


Figure 5. Sliding strip calculations. The T_k ($1 \leq k \leq 6$) are temporary matrices used inside the loop over i . At the end of the calculations (and hence just before the loop is incremented), the middle value (*i.e.* the $(w+1)^{\text{th}}$ value) from each T_k is transferred to a permanent array P_k . The FIT, DIFF and RESID operations are referred to in the text.

procedure. To reduce the diagram to as simple a form as possible, all technicalities arising solely from the NAG routines have been omitted. It is assumed that the reader is either familiar with the routines in question or can become familiar with them. By "technicalities" is meant such features as the routines working in terms of a normalised abscissa, \bar{x}

$$\bar{x} = \frac{2x - (x_{\max} + x_{\min})}{(x_{\max} - x_{\min})} \quad (18)$$

This sliding strip procedure is repeated for as many data points as possible. Obviously, it cannot be carried out on the points at the very beginning and very end of the data. In particular, if we use our above definition of each sliding strip consisting of $2w+1$ points (*i.e.* the central point and w points on either side), the method cannot be used for the first w and the last w points. Therefore, if we start with N (r^2 , $\ln J$) points then the maximum number of (r, M_w) points we can derive is $N-2w$. Once evaluated the sliding strip Chebyshev polynomials can be used to generate plots of point M_w versus r (or equivalently ξ) or point M_w versus C (or absorbance). MSTAR gives both and Fig. 6 gives an example for IgM using a sliding strip length of 13 (*i.e.* $w=6$). As would be expected, data of this type becomes more noisy near the meniscus or, equivalently, smaller values of $(C-C_a)$ where the concentration increments ΔC are small.

Point z-average Evaluations

The z-average (apparent) molecular weight is calculated from eq. (6b). When calculating the local slopes of $\ln C$ vs. r^2 , opportunity is also taken of doing the same for the (r, j) data (see Fig. 3). Thus, when it comes to calculating M_z , an array of

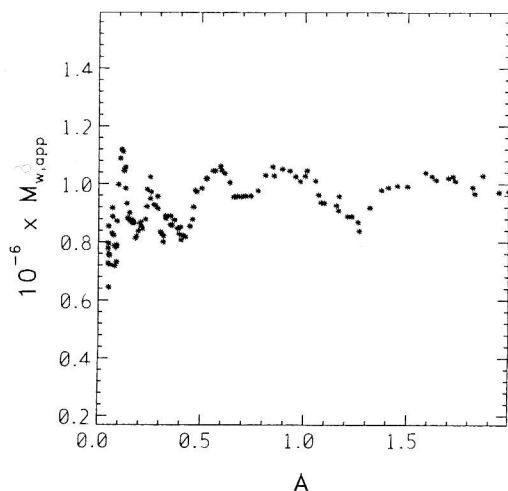


Figure 6. Plot of point weight average (apparent) molecular weight versus concentration (in absorbance units at 278 nm) for a low speed sedimentation equilibrium on human IgM₁ (other details as Fig. 4).

dC/dr values is already available (except that it is deficient in the first w and last w values). The second differentiation in eq. (6b) (*i.e.* with respect to r^2) is now carried out with another sliding strip procedure. For generality, the number of points used in each strip is $2z+1$ where z is another integer which is, in general, not equal to w . We have been using the default value $z=7$.

An important feature of eq. (6b) is that it shows that the $M_z(r)$ clearly do not depend on the value of J_a . However, because of the double differentiation in eq. (6a) (or (6b)), $M_{z,app}$ is very sensitive to data error and we have found so far that absorption optics do not provide reliable enough data for $M_{z,app}$ to be evaluated unless whole curve quadratic fitting to the data is used, with the usual risks of "oversmoothing".

5. MSTARI

MSTARI is similar to MSTARA except for two features. First, the data is taken from the analytical ultracentrifuge in the form of a photographic negative showing the fringes from the Rayleigh interferometer in the optical system. After this negative has been enlarged, the data are digitised on a gel scanner controlled from a PC. As noted above, data near the meniscus are generally unavailable or, at least, very noisy. The laser densitometer ANALYSE software (Chapter 5) incorporates a procedure to extrapolate the fringe data back to the meniscus. This obviates the need for a procedure equivalent to the calculation of I_{block} (see above and the Appendix) since by the time the data is presented to MSTARI it is already complete.

The second difference is that, as pointed out above, Rayleigh interferometry only gives concentration in relative units. These "fringe" units (j) are relative to the concentration at the meniscus (J_a). Thus, before starting the calculations, it is necessary to evaluate J_a . This is done by using the method leading up to eq. (16). Despite the problem of J_a evaluation (a problem which can be avoided *if* the high speed meniscus depletion method can be applied), data captured using Rayleigh interferometry tend to be more precise than that captured using absorption optics and so the $M_{z,app}(r)$ results are usually more realistic: Fig. 7¹² shows plots of $\ln J$ versus ξ , M^* versus ξ , M_w versus J and M_z versus J for a *relatively* "ideal" "monodisperse" system (colonic mucin T-domains); Fig. 8¹³ gives the corresponding set of plots for a very non-ideal system of xanthan.

6. MODE OF OUTPUT FROM MSTAR

The principle mode of output is graphical: For MSTARI this will be plots of $j/(r^2-a^2)$ versus $I/(r^2-a^2)$ and $J_{a,app}$ versus r in the initial running of the programme (to obtain an estimate for J_a) and plots of $\ln J$ versus ξ , M^* versus ξ , M_w versus J (and ξ) and M_z versus J (and the option of M_{y2} versus J). Estimates for J_a and $M^*(\xi \rightarrow 1)$ are usually best done by manual extrapolation (because of the perils of computer extrapolations of non-linear plots!). MSTARA produces plots of $\ln C$ (or A) versus ξ , M^* versus ξ , M_w versus ξ , M_w versus C (or A) and the option of M_{y2} versus C (or A). Both versions of MSTAR gives the option of printed output from the various calculation stages, including M^* , M_w and M_z versus ξ or C although with the large number of data points

involved (100 - 200), this can yield an unwieldy amount of output. The routine also however prints out an estimate for C_0 (the initial loading concentration in appropriate units) based on the usual conservation of mass equation:

$$\int_a^b C(r) dr = \frac{C_0 (b^2 + a^2)}{2} \quad (19)$$

and the comparison of this with the "expected" C_0 provides a useful check for possible errors.

7. MSTAR AND THERMODYNAMIC NON-IDEALITY

MSTAR makes no provision for calculating virial coefficients. All molecular weights are apparent values - *i.e.* corresponding to a finite concentration, C . However, for most systems at low loading concentrations (for proteins ≤ 1.0 mg/ml; polysaccharides ≤ 0.4 mg/ml), non-ideality effects can be negligible. In cases of severe non-ideality (as manifested by strong downward curvature of M_w versus C , A or J plots), a crude estimate for the "ideal" molecular weight can be obtained by extrapolating M_w (or the reciprocal thereof) back to zero C , A or J . For example, in the xanthan example of Fig. 7c, an "ideal" value for $M_w(J \rightarrow 0)$ of $\approx 3 \times 10^6$ could be inferred. This procedure can lead to underestimates however especially if there is significant re-distribution of the sample in very polydisperse materials, so some caution has to be expressed. The most rigorous - albeit time consuming - procedure is to measure $M_{w,app}^0$ (from $M^*(\xi \rightarrow 1)$ - see *e.g.* ref. 14) at a series of loading concentrations C_0 and extrapolate back to zero C_0 .

MSTAR *does* permit the input of a known thermodynamic (or "osmotic pressure") second virial coefficient B from which ideal M values can be calculated

$$\frac{1}{M} \approx \frac{1}{M_{app}} - 2BC \quad (20)$$

The M values in all the plots then refer to *ideal* molecular weights, not *apparent* ones.

8. MSTAR AND FLOTATION EQUILIBRIUM

For systems of macromolecules whose density is *less* than that of the solvent (*e.g.* lipoproteins in aqueous solvent or synthetic polymers in chloroform), the solute distribution at equilibrium will be opposite to that of the centrifugal field - *i.e.* flotation equilibrium. The situation for *low-speed* flotation equilibrium has been considered in ref. 15 and a version of MSTAR for this case is currently being written.

APPENDIX - CALCULATION OF 'BLOCK' FOR MSTARA

For MSTARA we need to calculate (for the evaluation of $M^*(r)$ via eq. (9)) the integral

$$2 \int_a^{r_1} r(C(r) - C_a) dr \equiv \int_a^{r_1} (C(r) - C_a) d(r^2)$$

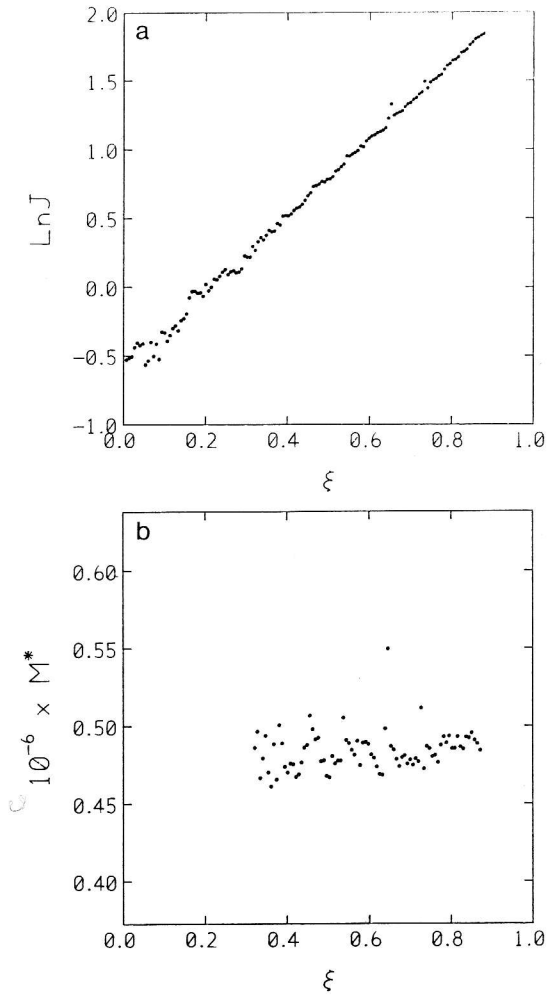


Figure 7. MSTARI analysis of solute low speed sedimentation equilibrium distribution data for colonic mucin T-domains. $M_{w,app}^0$ (from plot (b)) $\sim (0.50 \pm 0.02) \times 10^6$ g/mol. Loading concentration ~ 1.0 mg/ml. Solvent: phosphate/chloride buffer (pH=6.8, $I=0.10$). Rotor speed = 5200 rev/min; temperature = 20°C. (From ref. 12).

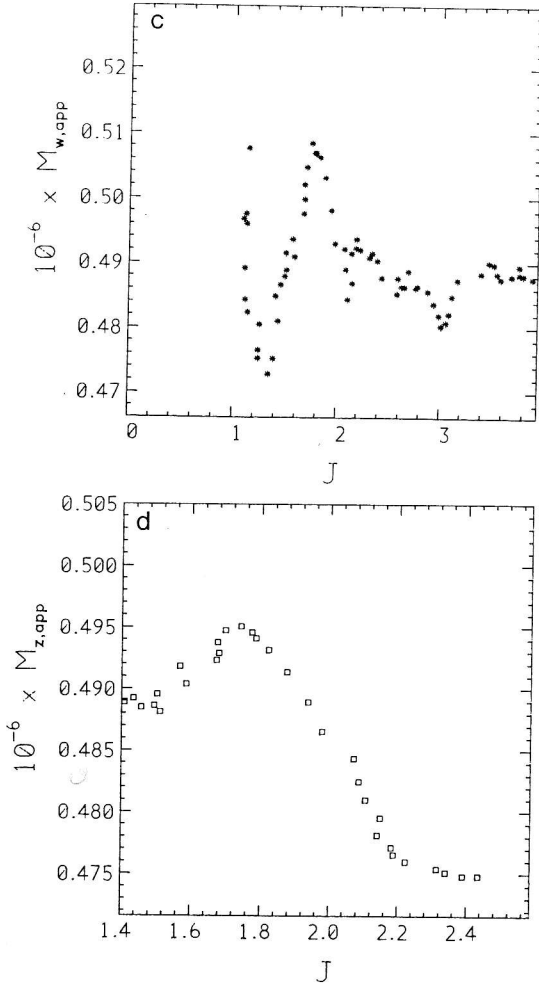


Figure 7 continued.

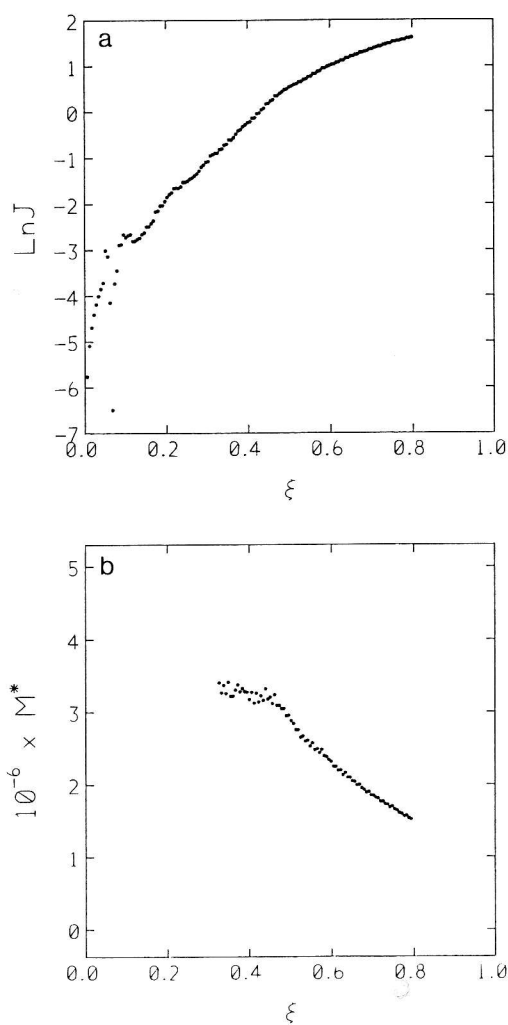


Figure 8. MSTARI analysis of solute (near meniscus depletion) sedimentation equilibrium distribution data for a highly non-ideal xanthan "RD" solution. $M_{w,app}^0$ (from plot (b)) $\sim (1.0 \pm 0.2) \times 10^6$ g/mol. Loading concentration ~ 0.5 mg/ml. Solvent: phosphate/chloride buffer (pH=6.8, $I=0.10$). Rotor speed = 3000 rev/min; temperature = 20.1°C. (From ref. 13.)

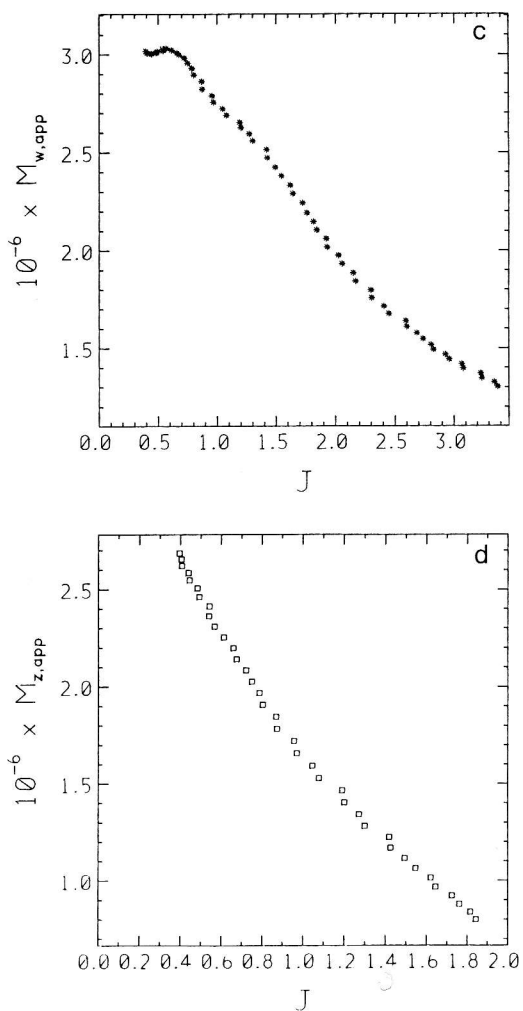


Figure 8 continued.

where C can either be in g/ml or in absorbance units.

$$\text{Let } I_{\text{block}} = \int_a^{r_1} (C(r) - C_a) d(r^2)$$

Assume $\ln C$ vs. r^2 is linear (reasonable for small $r_1 - a$)

$$\text{i.e. } \ln C(r) = X + Yr^2$$

$$\text{or } C(r) = \exp X \exp Yr^2$$

$$\begin{aligned} \text{Thus } I_{\text{block}} &= \int_a^{r_1} \{ \exp X \exp Yr^2 - C_a \} d(r^2) \\ &= \frac{\exp X}{Y} \{ \exp Yr_1^2 - \exp Ya^2 \} - C_a \{ r_1^2 - a^2 \} \end{aligned}$$

Also note:

$$C_a \equiv C(r=a) = \exp X \exp Ya^2$$

and

$$C_b \equiv C(r=b) = \exp X \exp Yb^2$$

REFERENCES

1. D. Roark and D.A. Yphantis, *Ann. N.Y. Acad. Sci.*, 1969, 164, 245.
2. M.L. Johnson, J.J. Correia, D.A. Yphantis and H.R. Halvorson, *Biophys. J.*, 1981, 36, 575.
3. T. Laue, Chapter 7, this volume.
4. H. Fujita, 'Foundations of Ultracentrifuge Analysis', J. Wiley and Sons, New York, 1975.
5. J.M. Creeth and R.H. Pain, *Prog. Biophys. Mol. Biol.*, 1967, 17, 217.
6. D.C. Teller, *Methods Enzymol.*, 1973, 27, 346.
7. J.M. Creeth and S.E. Harding, *J. Biochem. Biophys. Methods*, 1982, 7, 25.
8. H. Rinde, Ph.D. Thesis, 1928, Uppsala, Sweden.
9. J.M. Creeth, *Biochem. Soc. Trans.*, 1980, 8, 520.
10. D.C. Teller, J.A. Horbett, E.G. Richards and H.K. Schachman, *Anal. N.Y. Acad. Sci.*, 1969, 164, 66.
11. P.E. Gill and G.F. Miller, *Comput. J.*, 1972, 15, 80.
12. A. Allen, F. Fogg, S.E. Harding and N. Errington, in preparation.
13. N. Errington, J. Morgan and S.E. Harding, in preparation.
14. S.E. Harding, A.J. Rowe and J.M. Creeth, *Biochem. J.*, 1983, 209, 893.
15. S.E. Harding, P.J. Morgan and K. Petrak, *J. Phys. Chem.*, 1990, 94, 978.